Journal of Hazardous Materials 192 (2011) 1690–1696

Contents lists available at ScienceDirect

Journal of Hazardous Materials

journal homepage: www.elsevier.com/locate/jhazmat

Characteristics of diethylenetriamine-crosslinked cotton stalk/wheat stalk and their biosorption capacities for phosphate

Xing Xu, Yue Gao, Baoyu Gao*, Xin Tan, Ya-Qin Zhao, Qinyan Yue, Yan Wang

Key Laboratory of Water Pollution Control and Recycling (Shandong), School of Environmental Science and Engineering, Shandong University, Jinan 250100, PR China

ARTICLE INFO

Article history:
Received 15 April 2011
Received in revised form 17 June 2011
Accepted 1 July 2011
Available online 8 July 2011

Keywords:
Cotton stalk
Wheat stalk
Diethylenetriamine
Biosorbent
Phosphate

ABSTRACT

Two polymeric biosorbents were prepared from cotton stalk (CS) and wheat straw (WS) by the epichlorohydrin–diethylenetriamine–trimethylamine method. Amine-crosslinked cotton stalk (AC-CS) and wheat stalk (AC-WS) were used for the adsorption of phosphate, and their physicochemical properties as well as biosorption properties for phosphate were discussed intensively. Results indicated that the contents of holocellulose in CS and WS corresponded to the distinct phosphate adsorption capacities between AC-CS and AC-WS. Zeta potential and Raman spectra analysis illustrated the electrostatic attraction between phosphate ions and biosorbents. The adsorption of phosphate was not strongly pH dependent when the pH was about 4.0–9.0. The Langmuir isotherm provided the better fit and the maximum adsorption capacity (Q_{max}) was 51.54 mg/g for AC-CS and 60.61 mg/g for AC-WS. The saturated adsorption capacities of AC-CS and AC-WS in column were 49.05 and 41.9 mg/g, which accounted for about 80.3% and 81.4% of these biosorbents' Q_{max}. NaCl and HCl solutions demonstrated the excellent regeneration capacities for the biosorbents, and after three times of adsorption–desorption cycles, the column adsorption capacities of these biosorbents were still higher than 92%.

1. Introduction

Nitrogen and phosphorus are known as a significant nutrient to induce eutrophication, which is reported that phosphorus is especially limiting factor to control this phenomena [1]. Phosphorus is often present mainly at low concentrations in aqua-systems almost solely as phosphates, including organic phosphate, inorganic phosphate and polyphosphate [2]. Phosphate is released to aquatic environments through weathering of rocks and by various human activities such as industrial, agricultural and household uses [2,3]. The release of large amounts of phosphate-bearing wastes to surface water is of environmental concern, because it can stimulate the organisms and algaes growths in most ecosystems, which, in turn, have a harmful effect on fish and other aquatic life, resulting in deterioration of water quality [4].

Despite the environmental benefits of limiting nutrient release, there is a constant need to supply phosphorus to agriculture and industry. Thus, development of treatment methods that facilitate the removal of phosphate from wastewaters prior to discharge into natural waters is required. The broad categories of phosphate effluent treatment include physical, chemical, biological and crystallization methods [5–9]. Of all these, adsorption is well recognized as one of the simplest and safest methods used for the removal of pollutants from wastewater.

Studies on the adsorption of phosphate from wastewater before discharging into the environment have been carried out by using industrial waste materials and by-products as adsorbents, including fly ash [10], blast furnace slag [11] and iron oxide tailings [12]. In recent years, a new class of polymeric biosorbents was prepared from agricultural by-products for the adsorption of phosphate from wastewater, based on the appropriate chemical composition (cellulose and hemicellulose) in these agricultural by-products [13,14]. Cellulose and hemicellulose contain large amount of easily available hydroxyl groups, and these active hydroxyl groups can easily make a series of chemical reaction for polymeric ion exchanger preparation [15–17].

Polymeric biosorbents used in this work were prepared by the epichlorohydrin–diethylenetriamine–trimethylamine method by using cotton stalk and wheat stalk as starting materials, which were used as a source for natural cellulose fibers. Cotton and wheat stalks were thought as inexpensive materials which will be used as sorbents. The amine groups were introduced into these starting materials to form the amine-crosslinked cotton stalk (AC-CS) and amine-crosslinked wheat stalk (AC-WS). The AC-CS and AC-WS may show a distinction in their physicochemical and biosorption properties, ascribed to the distinct contents of cellulose and hemicellulose in raw cotton stalk (CS) and wheat straw (WS). The physicochemical properties of AC-CS and AC-WS were measured by elemental analysis, thermogravimetric analysis (TGA), zeta

* Corresponding author. Tel.: +86 531 88364832; fax: +86 531 88364513.
E-mail address: bygao@sdu.edu.cn (B. Gao).

0304-3894/$ – see front matter © 2011 Elsevier B.V. All rights reserved.
doi:10.1016/j.jhazmat.2011.07.009

Table 1
Chemical constitution of raw CS and WS.

Materials	Holocellulose (%)	Cellulose (%)	Hemicellulose (%)	Lignin (%)	Extractives (%)
Raw CS	49.5	23.6	25.9	25.3	19.5
Raw WS	61.3	32.1	29.2	16.4	16.9

potential analysis, BET surface analysis and Raman spectrum techniques. Biosorption properties of AC-CS and AC-WS were studied in static tests as well as in fixed-bed column tests at constant phosphate concentration of 100 mg/l and flow rate of 5 ml/min. In addition, the desorption capacities of these ion exchangers were evaluated after three times of adsorption–desorption cycles by using NaCl and HCl as the desorption eluents.

2. Materials and method

2.1. Biomass preparation, chemical modifications and characterization

2.1.1. Biomass preparation

The CS and WS were obtained from Zoupin, Shandong, China. The raw CS and WS were smashed into fragments with lengths of 0.2–1.0 cm, and thereafter these smashed agricultural by-products were washed with water and then dried at 60 °C for 24 h. The chemical constitution of CS and WS [18] are shown in Table 1. The higher holocellulose in raw WS suggests the more hydroxyl groups available in the amine reaction process.

2.1.2. Chemical modifications

The AC-CS and AC-WS were prepared by the epichlorohydrin–diethylenetriamine–trimethylamine method as follows: four grams of CS or WS were reacted with 10 ml of epichlorohydrin and 8 ml of N,N-dimethylformamide in a 250 ml three-neck round bottom flask at 90 °C for 45 min. Then 3.5 ml of diethylenetriamine was added and the mixture was stirred for 45 min at 90 °C, followed by adding 8 ml of triethylamine for grafting and stirring for 150 min at 90 °C. The product was washed with distilled water to remove the residual chemicals, dried at 105 °C for 6 h and then used in all the following bisorption experiments [8,19,20].

Cellulose monomer was used as the starting structure to show the synthesis scheme of the AC-CS and AC-WS as depicted in Fig. 1.

2.1.3. Characterization

TGA was carried out by a thermogravimetric analyzer (SHIMADZU, TGA-50) in order to determine the pyrolysis behavior of AC-CS and AC-WS. Samples were subjected to measure in the temperature range of 30–600 °C at heating rate 10 °C/min under flowing of nitrogen gas flow and held at 600 °C for 10 min. The nitrogen content of AC-CS/AC-WS was measured by using the element analyzer (Elementar Vario EL III, Germany) to evaluate the grafted functional groups in these biosorbents [8].

BET specific surface area was determined by the nitrogen adsorption isotherm technique, with an automatic BET surface area analyzer (Model F-Sorb 2400, Beijing Jinaipu Technical Apparatus Co., Ltd., China). The nitrogen adsorption was carried out at 77 K.

Zeta potential measurements were carried out using a microelectrophoresis apparatus (JS94H, Shanghai Zhongchen Digital Technical Apparatus Co., Ltd., China) to determine the zeta potentials of AC-CS/AC-WS and CS/WS. The samples' particles in the sediment phase were diluted with the upper clear liquid to make the particles visible under the microscope before measurement. The pH values of the suspensions were designed at pH range of 2.1–11.7.

Raman spectroscopy was used to explore the phosphate vibrational behaviors in the free and AC-CS/AC-WS-sorbed states. In the Raman analysis, to increase the signal-to-noise ratio, a highly concentrated phosphate solution was used with concentration of 5000 mg(P)/l phosphate. AC-CS/AC-WS (0.1 g) was added to the concentrated phosphate solution and mixed for 2 h at 180 rpm on a rotary mixer. In addition, the Raman spectra of phosphate ions in the AC-CS/AC-WS-sorbed states at different pH conditions were also measured by adjusting the concentrated phosphate solution in pH values of 2.1, 6.2 and 12.3, respectively.

The wet solid samples were analyzed by a Nicolet Almega XR Dispersive Raman spectrometer (Thermo Electron Corporation, USA). The laser wavelength used in Raman measurement was 1050 nm. Spectra were collected between 4000 and 400 cm^{-1}, with a resolution of 4 cm^{-1}. The exposure time was 2 s.

2.2. Chemicals

All the chemicals used in this study were of analytical grade. Inorganic chemicals: sulfuric acid, hydrochloric acid, sodium hydrate, ascorbic acid and ammonium molybdate; Organic chemicals: epichlorohydrin, diethylenetriamine, methanol, triethylamine, N,N-dimethylformamide were obtained from Sinopharm, China. The 1000 mg/l of phosphate stock solutions were prepared by dissolving 4.392 g of KH_2PO_4 (Deyang, China) in 1 l of distilled water.

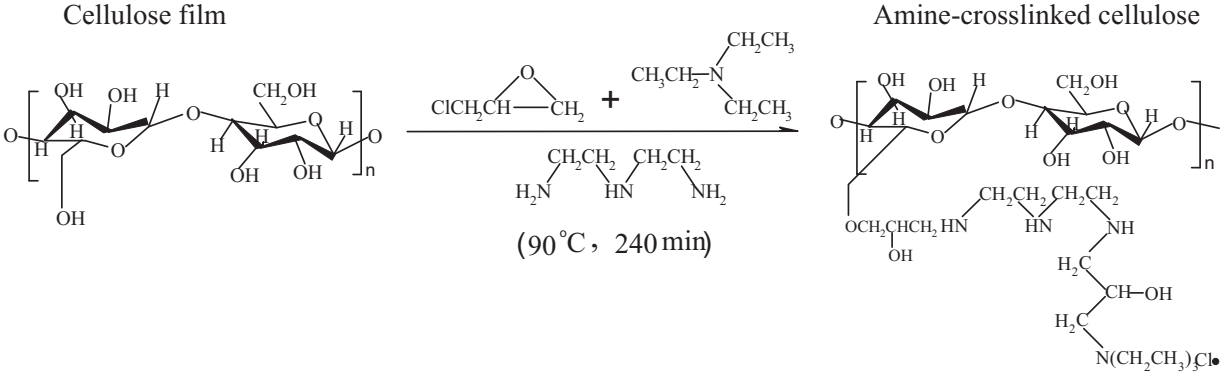

Fig. 1. Synthesis scheme of AC-CS and AC-WS using cellulose monomer as starting structure.

2.3. Biosorption experiments

Kinetic studies were carried out using 0.1 g AC-CS/AC-WS in 50 ml suspension containing 20, 30, and 50 mg(P)/l phosphate. Mixing was carried out at room temperature (20 °C) in 125 ml Erlenmeyer flasks at 180 rpm on a rotary mixer. Samples were drawn at 0, 1, 3, 5, 7, 10, 15, 20, 25, 30, 60 and 120 min, the last sampling time being sufficient to reach a steady state.

In the pH effect experiment, the initial pH of the phosphate solution (50 mg(P)/l) was first adjusted to 2.1, 4.2, 6.1, 9.3 and 11.8 by 1 mol/l of HCl and NaOH solutions, and then 0.1 g AC-CS/AC-WS was added to 50 ml of these solutions. Mixing was carried out at room temperature (20 ± 1 °C) in 125 ml Erlenmeyer flasks at 180 rpm on a rotary mixer and then the AC-CS/AC-WS and residual phosphate solutions were separated by 0.45 μm of microfiltration membrane. The residual concentration of each solution was determined at the wavelengths of UV-maximum (λ_{max}) at 700 nm by ammonium molybdate spectrophotometric method through a UV–visible spectrophotometer (model UV754GD, Shanghai).

The amounts of phosphate removed by AC-CS/AC-WS were determined by the following equation subscribed as:

$$q_e = \frac{V(C - C_e)}{m} \quad (1)$$

where q_e is the amount of adsorbed phosphate (mg/g); C_o and C_e are the original and equilibrium phosphate concentrations in solution (mg/l); V is the volume of the solution (l); m is the dosage of AC-CS/AC-WS (g).

2.4. Isotherm models

Isotherm tests were performed to determine AC-CS/AC-WS adsorption capacity for phosphate. AC-CS/AC-WS (0.1 g) was added to 50 ml tap water containing 20, 50, 100, 200, 250, 300, 400, 500, or 600 mg/l(P). Mixing was performed in 125 ml Erlenmeyer flasks placed on a rotary mixer at 180 rpm for 180 min to reach equilibrium at room temperature (20 ± 1 °C).

2.5. Column adsorption/desorption tests

Column adsorption/desorption tests were performed by using an organic-glass column with 200 mm length and 12 mm diameter. One gram of AC-CS/AC-WS was fed in the column and the flow rate of the influent (100 mg(P)/l) was controlled at about 5 ml/min. The effluent solutions were collected, and every 10 ml was selected as a sample to determine the concentrations of phosphate in the effluent solutions. The flow to the column was continued until the effluent phosphate concentration (C_t) approached the influent concentration (C_o), $C_t/C_o = 0.98$. Then, a dilute NaCl or HCl solution (0.1 mol/l) was eluted through the column for the desorption of phosphate from AC-CS/AC-WS. After washed with 100–500 ml of distilled water, the regenerated AC-CS/AC-WS were used again in the subsequent experiments. The adsorption and desorption cycles were repeated for several times and the concentrations of phosphate in the solution during adsorption and desorption were continuously monitored with an UV–visible spectrometer.

2.6. Statistical analysis

All adsorption experiments (except column adsorption and desorption tests) were replicated three times and only mean values were presented. All data were processed by origin 7.5, and the regression and the analysis of variance (one-way ANOVA) were conducted using the statistical programs of SPSS V13.0 (SPSS Inc., Chicago, IL). Significant levels were set at $\alpha = 0.05$.

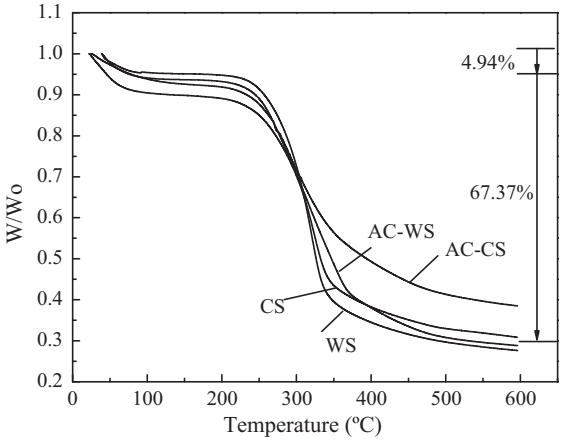

Fig. 2. TGA curves of AC-CS and CS/WS.

3. Results and discussion

3.1. Characteristics of the AC-CS/AC-WS

3.1.1. TGA of AC-CS/AC-WS

Thermograms obtained from the TGA of the CS as well as AC-CS are shown in Fig. 2. The loss of weight during the TG analysis of CS can be divided into three stages. The first weight loss (~4.94%) during the temperature range from 38 to 200 °C may be due to the moisture elimination. The second stage of 200–325 °C corresponds to primary carbonization, which has a major weight loss (67.37%). It is observed in Fig. 2 that the weight loss variation curve for the AC-CS shows a slight and continuous decrease when compared to the CS in this temperature range; this indicates that the grafted chemicals will have a certain degree of effect on the pyrolysis behavior of CS [21]. The third stage in the 325–600 °C range indicates the decomposition of a structure with higher stability. Similar results were observed in TGA curves of WS and AC-WS as shown in Fig. 2. This result was also reported in the work of Aravindhan for the TG analysis of activated carbon prepared from marine macro-algal biomass [22].

3.1.2. Elemental and surface characteristics analysis

Table 2 shows the elemental changes of AC-CS and AC-WS by compared with those of raw CS and WS. It is shown that the carbon contents, hydrogen contents and nitrogen contents in raw materials are about 41.11–41.34%, 6.10–6.70% and 0.35–0.97%, respectively. After epichlorohydrin–diethylenetriamine–trimethylamine modification, a significant increase in the nitrogen content is observed in both of the compositions of AC-CS (0.97–6.98%) and AC-WS (0.35–8.45%); this indicates that large amounts of amine groups have been crosslinked into the structure of cellulose chains, resulting in the increase of nitrogen content in these biosorbents. In addition, the higher nitrogen content observed in AC-WS illustrates the existence of more amine groups in structure of AC-WS, which validates the superiority of raw WS in amine reaction process.

The BET surface areas of raw CS, WS, AC-CS and AC-WS are also shown in Table 2. The BET surface areas of AC-CS (5.68 m^2/g)

Table 2
Change of elemental content and BET surface areas.

	N (%)	C (%)	H (%)	BET surface areas (m^2/g)
CS	0.32	41.34	6.70	6.58
WS	0.35	41.11	6.10	8.82
AC-CS	6.98	42.34	6.82	5.68
AC-WS	8.45	43.25	7.2	6.49

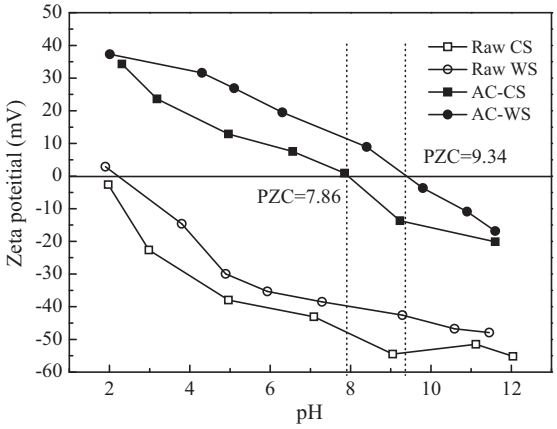

Fig. 3. Zeta potentials of raw CS, WS, AC-CS and AC-WS as a function of pH.

and AC-WS (6.49 m^2/g) are lower than those of raw CS (6.58 m^2/g) and WS (8.82 m^2/g). Apparently, crosslinking of amine groups onto the raw CS and WS leads to a constriction of the pore channels, as a result of attachment of these chemical reagents to the internal framework surfaces. Similar reduction in the BET surface area was also observed during the modification of coconut coir with hexadecyltrimethylammonium [23].

3.1.3. Zeta potential analysis

The effect of functionalization with amine functional group and pH on the surface charges of AC-CS and AC-WS was studied by comparing those of raw CS and WS (Fig. 3). It is observed that the Zeta potentials of raw CS and WS are much lower than those of AC-CS and AC-WS. The increased Zeta potentials in AC-CS and AC-WS indicate that amine functional groups are incorporated onto the framework of AC-CS and AC-WS, which increases the surface potential of these biosorbents. These findings are in agreement with the reported work shown in [9,24,25].

The Zeta potential of raw CS decreases from −2.54 to −42.2 mV as the pH increases from 2.3 to 12.1, whereas the Zeta potential of AC-CS decreases from +34.1 to −20.7 mV as the pH increases from 2.1 to 12.0. Similar trends were also shown in the curves of the AC-WS and raw WS. The decreased Zeta potentials of AC-CS/AC-WS and raw CS/WS could be attributed to the pH-dependent functional groups existing in AC-CS/AC-WS and raw CS/WS, such as hydroxyl and carboxyl groups. These groups will exhibit a greater negative charge as the pH increases and result in the decrease of the positive charge in these samples.

The point of zero charge (PZC) for AC-CS is 7.86, whereas the PZC for AC-WS is 9.34. The higher PZC for AC-WS indicates the more pH-independence of AC-WS as compared with that of AC-CS.

3.1.4. Raman spectroscopy

Raman analysis was used to examine the interaction between phosphate ions and AC-CS/AC-WS by probing the shifts in the stretching bands when aqueous phosphate ions were adsorbed onto these biosorbents. The symmetric stretching vibration band (υ_1) of the anion is commonly measured because its position varies with ion association and ion–ion interactions. In our previous work, the spectra of the (υ_1) mode for phosphate in many phases were recorded to provide insights into the mechanisms of phosphate interactions with other adsorbents [7].

Raman spectra of aqueous phosphate ions and phosphate-loaded biosorbents are presented in Fig. 4. A Raman peak for phosphate in a 0.2 mol/l of KH_2PO_4 solution (pH: 6.2) was detected at 898 cm^{-1}. The peaks of the adsorbed phosphate in AC-CS and AC-WS are at 895 cm^{-1} and 896 cm^{-1}, respectively. These peaks agree with the characteristic peak of the free phosphate ion in solution. The similar band position of the soluble and adsorbed phosphate shows no strong chemical interaction between the adsorbed phosphate and AC-CS/AC-WS. The reported data in our previous work showed that the phosphate peak detected on a geed based biosorbent was at 896 cm^{-1}, which agreed with the results in this work [7,25].

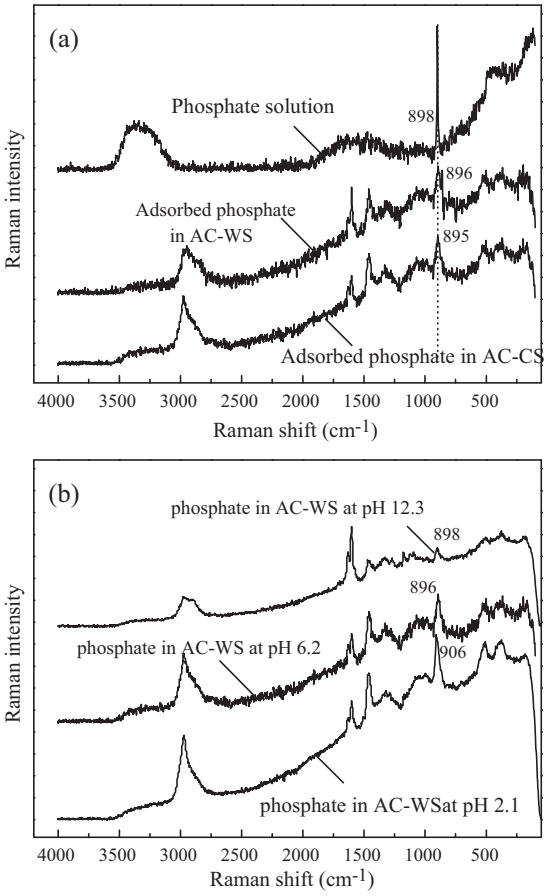

Fig. 4. Raman spectrums of (a) aqueous phosphate solution, adsorbed phosphate in AC-SW and AC-CS; (b) phosphate in AC-WS at pH 2.1, 6.2 and 12.3.

The effects of pH on the Raman spectra of the adsorbed phosphate were studied by detecting the peak positions (adsorbed phosphate in AC-WS) at pH 2.1, 6.2 and 12.3. The peaks of the adsorbed phosphate at pH 2.1, 6.2 and 12.3 are at 906 cm^{-1}, 896 cm^{-1} and 898 cm^{-1}, respectively. At neutral and alkalic conditions, the phosphate ions exist in the form of $H_2PO_4^-$, HPO_4^{2-} and PO_4^{3-}, which could be adsorbed onto the amine sites by electrostatic attraction [25]. As a result, the peaks of the adsorbed phosphate at pH 6.2 and 12.3 have a negligible frequency shift of ~1–2 cm^{-1}.

Adsorption of phosphate onto the biosorbents at pH 2.1 results in a relatively large peak shift to 906 cm^{-1}, suggesting that phosphate is associated on the biosorbents surface through interactions stronger than electrostatic forces. At pH 2.1, the main form of phosphate is H_3PO_4. The shift of peak at 906 cm^{-1} corresponds to the bonding between H_3PO_4 and adsorption sites. This result also indicates that phosphate ion association in the phosphate–biosorbents system was not pH-independent at pH 2.1. Similar result was reported in the work of Yoon for perchlorate adsorption and desorption on activated carbon and anion exchange resin [24].

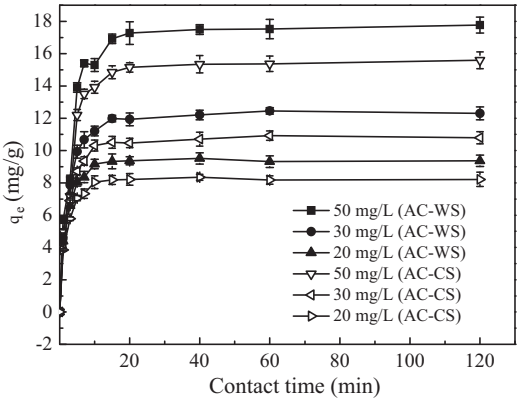

Fig. 5. Kinetic studies of AC-WS and AC-CS for phosphate versus the contact time.

3.2. Adsorption tests for phosphate

3.2.1. Kinetic studies

The adsorption capacities of AC-WS and AC-CS for phosphate versus the contact time are shown in Fig. 5. The experimental data were measured at 2 h to make sure that full equilibrium was attained. As shown in Fig. 5, for all phosphate concentrations and biosorbents, the amount of phosphate adsorbed q_t at time t increases with time and the adsorption reaches an equilibrium q_e within 15 min. Two distinct adsorption stages were observed before the equilibrium stage. Stage 1 (1–5 min), represented by a steep slope, reflects a rapid adsorption rate with uptake of 70–80% of phosphate. The extremely rapid adsorption process occurs in stage 1 could be attributed to instantaneous monolayer adsorption of phosphate at the biosorbent surface [26]. Stage 2 (5–15 min), signified by a gentle slope, is characterized by a gradually reduced adsorption rate prior to reaching equilibrium. The decreased adsorption rate in stage 2 reflects rearrangement of phosphate adsorbed on the surface of these biosorbents and a more thorough utilization of adsorption sites [24]. After 15 min, the system reaches an equilibrium state (stage 3).

3.2.2. Effect of pH

Fig. 6 shows the effect of pH on the adsorption of phosphate by AC-CS/AC-WS. It shows that the pH value of the phosphate solution plays an important role in the whole adsorption process and particularly on the adsorption capacity. The adsorption capacity is not strongly pH dependent when the pH is about 4.0–9.0, i.e. capacity keeps almost constant in this range. However, below a pH value of about 4 the capacity decreases due to the function of protonation caused by the high concentration of H^+ at acidic condition. When the pH increases to 12.0, the capacity significantly decreases to an upper state, attributed to the abundance of OH^- and the less attractive or more repulsive electrostatic interaction at higher solution pH values.

When the adsorption reaches an equilibrium state, the original pH values (2.1, 4.2, 6.1, 9.3 and 11.7) are shifted to 2.40, 4.34, 6.23, 6.76, 8.78 for AC-CS and 2.44, 4.29, 6.16, 7.01, 8.35 for AC-WS. It shows a neutral trend for all the pH values after the adsorption process; this may be attributed to the species of phosphate ions in aqueous solution (i.e. H_3PO_4, $H_2PO_4^-$, HPO_4^{2-} and PO_4^{3-}), which form a buffer solution during adsorption process.

3.2.3. Isotherm tests

Fig. 7 shows the adsorption equilibrium results of AC-CS and AC-WS for phosphate. Equilibrium results (Fig. 7) were tested for fit with the Langmuir and Freundlich models. The Langmuir model assumes monolayer adsorption with maximum adsorption upon

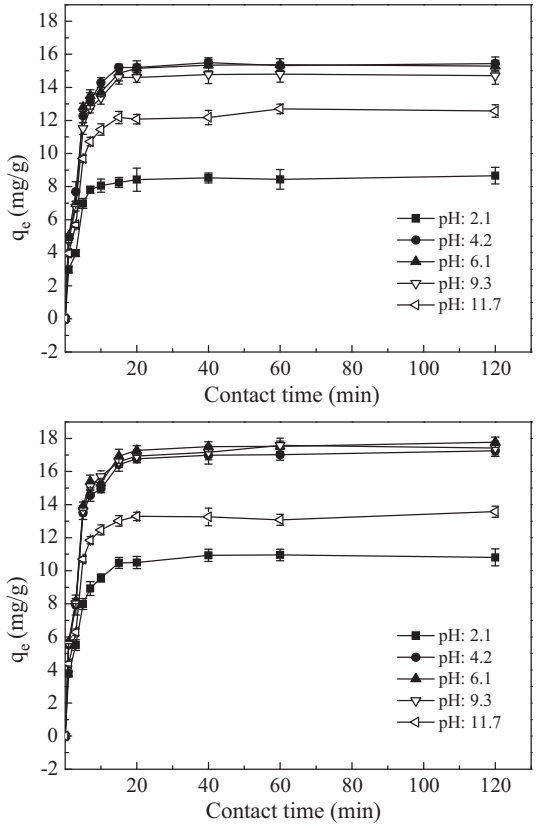

Fig. 6. Effect of pH on the adsorption of phosphate by AC-CS/AC-WS.

monolayer saturation, no interaction between the adsorbed anions species, and constant adsorption energy on all sites. The Langmuir model [27–29] is described by Eq. (2):

$$\frac{1}{q_e} = \frac{1}{Q_{max}} + \frac{1}{bQ_{max}}\frac{1}{C_e} \quad (2)$$

where Q_{max} is the maximum adsorption capacity (mg/g) and b is Langmuir constant (1/mg).

The Freundlich model assumes that the adsorbent surface is heterogeneous with multiple adsorption layers. In this model, the maximum adsorption capacity is not defined and adsorption energy

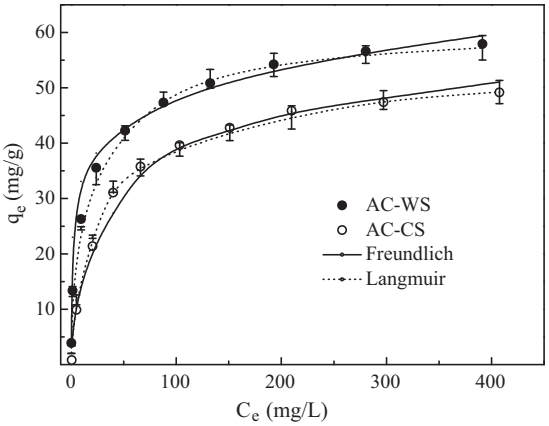

Fig. 7. Adsorption equilibrium results and the fitted Langmuir and Freundlich isotherm model.

Table 3
Isotherm parameters for adsorption phosphate by AC-WS/AC-CS.

Biosorbents	Langmuir			Freundlich		
	Q_{max} (mg/g)	b (l/mg)	R^2	K_F ((mg/g)/(mg/l))	n	R^2
AC-WS	60.61	0.043	0.991	7.87	2.47	0.985
AC-CS	51.54	0.032	0.992	7.30	2.40	0.983

Table 4
Q_{max} of PO_4^{3-} for different adsorbents.

Adsorbents	Q_{max} (mg/g) PO_4^{3-}(P)	References
AC-CS	51.54	This work
AC-WS	60.61	This work
Giant reed based resin	54.67	[20]
Corn stalk based resin	40.48	[33]
Actived carbon	6.8	[34]
Commercial anion exchange resins	13.8–42.1	[6,34]

varies among adsorption sites. The Freundlich model [30–32] is described by Eq. (3):

$$\ln\ q_e = \ln K_F + \frac{1}{n} ln\, C_e \quad (3)$$

where K_F is the Freundlich constant relating to the strength of adsorbate–sorbent interactions [(mg/g)/(mg/l)], and n is a dimensionless exponent between 0 and 1 relating to the degree of surface heterogeneity.

Parameters of the two isotherms are summarized in Table 3. The Langmuir isotherm provides the better fit as it has the higher correlation coefficient (R^2 = 0.989). Better fit values for AC-CS were: Q_{max} = 51.54 mg/g and b = 0.032 l/mg; for AC-WS were: Q_{max} = 60.61 mg/g and b = 0.043 l/mg. It shows that the adsorption capacity of AC-WS is higher than that of AC-CS, indicating the stronger interaction between phosphate ions and AC-WS. This result further validates the superiority of raw WS in biosorbent preparation due to the higher holocellulose in its constituent.

Some others lingo cellulosic biomasses [20,33] as well as some commercially available adsorbents' adsorption capacities [6,34] for phosphate are shown in Table 4. It is shown that the phosphate adsorption capacities of AC-WS (60.61 mg/g) and AC-CS 51.54 (mg/g) are higher than those of giant reed based resin (54.67 mg/g), corn stalk based resin (40.48 mg/g), actived carbon (6.8 mg/g) and some commercial anion exchange resins (13.8–42.1 mg/g); this indicates that the biosorbents prepared in this study can be considered as the alternative materials for phosphate removal in aqueous solution.

The essential feature of the Langmuir isotherm can be expressed by means of a dimensionless constant separation factor or equilibrium parameter R_L, which could indicate the effect of the isotherm shape on the favorability of adsorption. R_L is calculated using Eq. (4) [35]:

$$R_L = \frac{1}{1 + bC_o} \quad (4)$$

$R_L > 1$ for unfavorable adsorption, $R_L = 1$ for linear adsorption, $0 < R_L < 1$ for favorable adsorption, and $R_L = 0$ for irreversible adsorption. The better-fit Langmuir parameters yield R_L <1, indicating favorable uptake of phosphate by AC-WS and AC-CS.

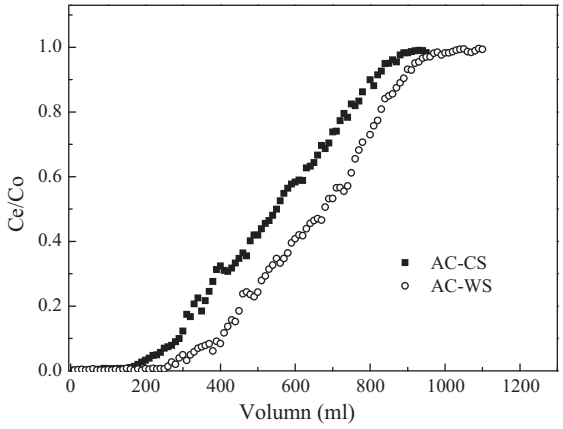

Fig. 8. Column adsorption of phosphate by AC-WS and AC-CS.

3.2.4. Column adsorption and desorption tests

The results in Fig. 8 present the column adsorption of phosphate by AC-WS and AC-CS. The influent solution was infused into the columns with biosorbents of 1 g, phosphate concentration of 100 mg/l and flow rate of 5 ml/min. It is observed that the breakthrough volumes (C_t/C_o = 0.1) for AC-WS and AC-CS are 360

Table 5
Desorption efficiencies of desorption agents for the biosorbents.

Biosorbents	Cycles	HCl		NaCl	
		Q_c (mg/g)	Efficiency (%)	Q_c (mg/g)	Efficiency (%)
AC-CS	Original	41.90	–	41.90	–
	1	41.22	98.4	40.64	97.1
	2	40.43	96.5	39.93	95.3
	3	38.96	93.1	38.67	92.3
AC-WS	Original	49.05	–	49.05	–
	1	48.45	98.9	48.04	98.2
	2	46.94	95.8	47.89	97.7
	3	45.90	93.7	46.55	95.0

and 270 ml, respectively. As the phosphate solution continues to flow into the columns, the points on the S-shaped curve gradually approach their exhaustion values ($C_t/C_o = 0.98$). When the effluent phosphate concentration reaches the influent concentration, the saturated adsorption capacities of AC-WS and AC-CS in column are 49.05 and 41.90 mg/g, respectively, which account for about 80.3% and 81.4% of the Q_{max} of these biosorbents (Q_{max} for AC-WS: 60.61 mg/g; Q_{max} for AC-CS: 51.54 mg/g).

Elution of the adsorbed phosphate ions and repeated usability of the biosorbents are important in reference to the practical applications of treatment of industrial effluent. In this work, 0.1 mol/l NaCl or HCl solution was selected for the regeneration of the two biosorbents. After three adsorption–desorption cycles, it is observed that the regeneration capacities for these biosorbents are still higher than 92% (Table 5). It seems that the desorption of phosphate ions from the AC-WS and AC-CS is most probably through an reaction of ion-exchange by the reverse of the reactions with Cl^- from the NaCl or HCl solution displacing phosphate ions from the biosorbents.

However, a weight loss (about 5%) of the biosorbents is observed after using HCl as eluent. Similar result was reported by Osifo [36] who observed a weight loss (25%) of chitosan beads by using HCl solution as the desorption agent, ascribed to the destruction of cellulose and hemicellulose in biosorbents caused by the corrosion of HCl solution.

4. Conclusions

AC-CS and AC-WS were prepared for the adsorption of phosphate in this work. Amine groups in these biosorbents were detected after the characteristic analysis and the Q_{max} of AC-CS and AC-WS for phosphate were 51.54 mg/g and 60.61 mg/g. Zeta potential and Raman spectrum analysis illustrated the electrostatic attraction between phosphate ions and biosorbents. The adsorption of phosphate was not strongly pH dependent when the pH was about 4.0–9.0. The saturated adsorption capacities of AC-CS and AC-WS in column are 41.9 and 49.05 mg/g. In addition, the biosorbents could be regenerated by using 0.1 mol/l NaCl or HCl solution as eluent, and the regeneration capacities for these biosorbents were still higher than 92% after three adsorption–desorption cycles.

Acknowledgments

The research was supported by the National Natural Science Foundation of China (50878121 and 21007034) and National Major Special Technological Programmes Concerning Water Pollution Control and Management in the Eleventh Five-year Plan Period (2008ZX07010-008-002).

References

[1] M. Özacar, Adsorption of phosphate from aqueous solution onto alunite , Chemosphere 51 (4) (2003) 321–327.
[2] J. Das, B.S. Patra, N. Baliarsingh, K.M. Parida, Adsorption of phosphate by layered double hydroxides in aqueous solutions , Appl. Clay Sci. 32 (2006) 252–260.
[3] E. Oguz, Removal of phosphate from aqueous solution with blast furnace slag , J. Hazard. Mater. 114 (2004) 131–137.
[4] K. Karageorgiou, M. Paschalis, G.N. Anastassakis, Removal of phosphate species from solution by adsorption onto calcite used as natural adsorbent , J. Hazard. Mater. 139 (2007) 447–452.
[5] S.S. Sablani, M.F.A. Goosen, Al-Belushi, M. Wilf, Concentration polarization in ultrafiltration and reverse osmosis: a critical review , Desalination 141 (2001) 269–289.
[6] K. Suzuki, Y. Tanaka, T. Osada, M. Waki, Removal of phosphate, magnesium and calcium from swine wastewater through crystallization enhanced by aeration , Water Res. 36 (2002) 2991–2998.
[7] X. Xu, B.Y. Gao, Q.Y. Yue, Q.Q. Zhong, Sorption of phosphate onto giant reed based adsorbent: FTIR, Raman spectrum analysis and dynamic sorption/desorption properties in filter bed , Bioresour. Technol. 102 (2011) 5278–5282.
[8] X. Xu, B.Y. Gao, Q.Y. Yue, Q.Q. Zhong, Preparation of agricultural by-product based anion exchanger and its utilization for nitrate and phosphate removal , Bioresour. Technol. 101 (2010) 8558–8564.
[9] S.U. Hong, L. Ouyang, M.L. Bruening, Recovery of phosphate using multilayer polyelectrolyte nanofiltration membranes , J. Membr. Sci. 327 (2009) 2–5.
[10] M.Y. Can, E. Yildiz, Phosphate removal from water by fly ash: factorial experimental design , J. Hazard. Mater. 135 (2006) 165–170.
[11] L. Johansson, J.P. Gustafsson, Phosphate removal using blast furnace slags and opoka-mechanisms , Water Res. 34 (2000) 259–265.
[12] L. Zeng, X.M. Li, J.D. Liu, Adsorptive removal of phosphate from aqueous solutions using iron oxide tailings , Water Res. 38 (2004) 1318–1326.
[13] A. Biswas, B.C. Saha, J.W. Lawton, R.L. Shogren, J.L. Willett, Process for obtaining cellulose acetate from agricultural by-products , Carbohydr. Polym. 64 (2006) 134–137.
[14] M.M. Ibrahim, A. Dufresne, W.K. El-Zawawy, F.A. Agblevor, Banana fibers and microfibrils as lignocellulosic reinforcements in polymer composites , Carbohydr. Polym. 81 (2010) 811–819.
[15] D.D. Andjelkovic, M. Valverde, P. Henna, F.K. Li, R.C. Larock, Novel thermosets prepared by cationic copolymerization of various vegetable oils – synthesis and their structure–property relationships , Polymer 46 (2005) 9674–9685.
[16] R. Ojah, S.K. Dolui, Graft copolymerization of methyl methacrylate onto Bombyx mori initiated by semiconductor-based photocatalyst , Bioresour. Technol. 97 (2006) 1529–1535.
[17] U.S. Orlando, T. Okuda, W. Nishijima, Chemical properties of anion exchangers prepared from waste natural materials , React. Funct. Polym. 55 (2003) 311–318.
[18] G.Z. Sheng, L. Li, The composition and properties of cotton-straw peer , J. Xian Polytech. Univ. 23 (2009) 18–23.
[19] X. Xu, B.Y. Gao, Q.Q. Zhong, Q.Y. Yue, Q. Li, Sorption of nitrate onto amine-crosslinked wheat straw: characteristics, column sorption and desorption properties , J. Hazard. Mater. 186 (2011) 206–211.
[20] X. Xu, B.Y. Gao, Q.Q. Zhong, Q.Y. Yue, Sorption of phosphate onto giant reed based adsorbent: FTIR, Raman spectrum analysis and dynamic sorption/desorption properties in filter bed , Bioresour. Technol. 102 (2011) 5278–5282.
[21] C.Y. Yin, J.B. Li, Q. Xu, Q. Peng, Y.B. Liu, X.Y. Shen, Chemical modification of cotton cellulose in supercritical carbon dioxide: synthesis and characterization of cellulose carbamate , Carbohyd. Polym. 67 (2007) 147–154.
[22] R. Aravindhan, J.R. Rao, B.U. Nair, Preparation and characterization of activated carbon from marine macro-algal biomass , J. Hazard. Mater. 162 (2009) 688–694.
[23] C. Namasivayam, M.V. Sureshkumar, Removal of chromium(VI) from water and wastewater using surfactant modified coconut coir pith as a biosorbent , Bioresour. Technol. 99 (2008) 2218–2225.
[24] I.H. Yoon, X. Meng, C. Wang, K.W. Kim, S. Bang, E. Choe, L. Lippincott, Perchlorate adsorption and desorption on activated carbon and anion exchange resin , J. Hazard. Mater. 164 (2009) 87–94.
[25] S. Baidas, B.Y. Gao, X.G. Meng, Perchlorate removal by quaternary amine modified reed , J. Hazard. Mater. 189 (2011) 54–61.
[26] Y. Wang, B.Y. Gao, W.W. Yue, Q.Y. Yue, Adsorption kinetics of nitrate from aqueous solutions onto modified wheat residue , Colloids Surf. A 308 (2007) 1–5.
[27] A. Sari, M. Tuzen, Biosorption of Pb(II) and Cd(II) from aqueous solution using green alga (Ulva lactuca) biomass , J. Hazard. Mater. 152 (2008) 302–308.
[28] A. Sari, M. Tuzen, Biosorption of cadmium(II) from aqueous solution by red algae (*Ceramium virgatum*): equilibrium, kinetic and thermodynamic studies , J. Hazard. Mater. 157 (2008) 448–454.
[29] A. Sari, M. Tuzen, Equilibrium, thermodynamic and kinetic studies on aluminum biosorption from aqueous solution by brown algae (*Padina pavonica*) biomass , J. Hazard. Mater. 171 (2009) 973–979.
[30] H. Freundlich, Colloid and Capillary Chemistry , Methuen & Co., London, 1926.
[31] A. Sari, M. Tuzen, Biosorption of total chromium from aqueous solution by red algae (*Ceramium virgatum*): equilibrium, kinetic and thermodynamic studies , J. Hazard. Mater. 160 (2008) 349–355.
[32] M. Tuzen, A. Sarı, D. Mendil, O.D. Uluozlu, M. Soylak, M. Dogan, Characterization of biosorption process of As(III) on green algae Ulothrix cylindricum , J. Hazard. Mater. 165 (2009) 566–572.
[33] Y. Wang, B.Y. Gao, W.W. Yue, X.M. Xu, X. Xu, Adsorption kinetics of phosphate from aqueous solutions onto modified corn residue , Environ. Sci. 29 (2008) 703–708.
[34] H.J. Park, C.K. Na, Preparation of anion exchanger by amination of acrylic acid grafted polypropylene nonwoven fiber and its ion-exchange property , J. Colloid Interface Sci. 301 (2006) 46–54.
[35] K.R. Hall, L.C. Eagleton, A. Acrivos, T. Vermeulen, Pore and solid diffusion kinetics in fixed-bed adsorption under constant pattern conditions , Ind. Eng. Chem. Res. Fund. 5 (1966) 212–223.
[36] P.O. Osifo, H.W.J.P. Neomagus, R.C. Everson, A. Webster, M.A. vd Gun, The adsorption of copper in a packed-bed of chitosan beads: modeling, multiple adsorption and regeneration , J. Hazard. Mater. 167 (2009) 1242–1245.